Generalizing Lambert's Law For Smooth Surfaces

Lawrence B. Wolff

Computer Vision Laboratory, Department of Computer Science, The Johns Hopkins University,Baltimore, Maryland 21218

Abstract. One of the most common assumptions for recovering object features in computer vision and rendering objects in computer graphics is that diffuse reflection from materials is Lambertian. This paper shows that there is significant deviation from Lambertian behavior in diffuse reflection from *smooth* surfaces not predicted by existing reflectance models, having an important bearing on any computer vision technique that may utilize reflectance models including shape-from-shading and binocular stereo. Contrary to prediction by Lambert's Law, diffuse reflection from smooth surfaces is significantly viewpoint dependent, and there are prominent diffuse reflection maxima effects occurring on objects when incident point source illumination is greater than 50° relative to viewing including the range from 90° to 180° where the light source is behind the object with respect to viewing. Presented here is a diffuse reflectance model, derived from first physical principles, utilizing results of radiative transfer theory for subsurface multiple scattering together with Fresnel attenuation and Snell refraction at a smooth air-dielectric surface boundary. A number of experimental results are presented demonstrating striking deviation from Lambertian behavior predicted by the proposed diffuse reflectance model.

1 Introduction

A prevalent class of materials encountered both in common experience and in computer vision/robotics environments are inhomogeneous dielectrics which include plastics, ceramics, and, rubber. In computer vision a widely used assumption about diffuse reflection from materials is Lambert's law [13], namely the expression:

$$\frac{1}{\pi} L \rho \cos\psi d\omega$$

where light is incident with radiance L, at incidence angle ψ, and reflected through a small solid angle $d\omega$, and ρ is termed the *diffuse albedo* in the range $[0, 1.0]$. This reflectance model is typically instantiated into the implementation of a large number of algorithms such as shape-from-shading [9] and photometric-based binocular stereo [6], [19]. It is therefore important for researchers in the computer vision community who utilize assumptions about diffuse reflection to be aware of the conditions under which there is significant deviation from Lambert's law.

Almost all diffuse reflection from inhomogeneous dielectrics physically arises from subsurface multiple scattering of light caused by subsurface inhomogeneities in index of refraction. In this paper we model inhomogeneous dielectric material as a collection of scatterers contained in a uniform dielectric medium with index of refraction different from that of air. An expression is derived for diffuse reflected radiance resulting from the process of incident light refracting into the dielectric medium across a smooth surface boundary, producing a subsurface diffuse intensity distribution from multiple internal scattering, and then refraction of this subsurface diffuse intensity distribution back out into air. See Figure 1. Also accounted for is the infinite progression of internal specular reflection at the air-dielectric boundary and sub-surface scattering. A common property of diffuse reflection from smooth inhomogeneous dielectric surfaces is that such reflection is azimuth independent with respect to viewing about the surface normal, regardless of the fixed direction of incident light. We formally derive and empirically verify that for smooth inhomogeneous dielectric surfaces that exhibit such azimuth symmetric diffuse reflection, that

$$\varrho L \times (1 - F(\psi, n)) \times \cos\psi \times (1 - F(\sin^{-1}(\frac{\sin\phi}{n}), 1/n))\, d\omega \qquad (1)$$

describes the reflected radiance into viewing angle, ϕ, (i.e., angle between viewing and the surface normal, also known as *emittance angle*). The terms $F(,)$ refer to the Fresnel reflection coefficients [18], n, is the index of refraction of the dielectric medium, and, ϱ, is the *total diffuse albedo*. We show that the total diffuse albedo, ϱ, is directly related to both the *single scattering albedo* describing the proportion of energy reradiated upon each subsurface single scattering, and, the index of refraction n. An initial first order derivation of expression 1 was presented in [23], however without the accounting for higher order effects which is presented below.

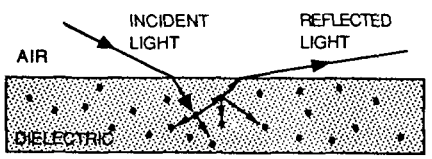

Figure 1

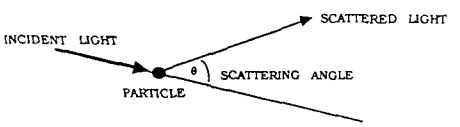

Figure 2

Particularly useful to object feature extraction in computer vision, our expression 1 for diffuse reflection allows precise characterization of the conditions under which the Lambertian model breaks down for inhomogeneous dielectrics and where our more accurate model should be used. We show that Lambert's law is valid for smooth dielectrics to within 5% only as long as both angle of incidence, ψ, and viewing angle, ϕ, are simultaneously less than $50°$. This means that for applications in computer vision there are a large number of situations in which Lambert's law is significantly in error for smooth surfaces– near the occluding contour of objects under any illumination condition; for illuminations

incident at greater than 50^o relative to viewing there will be significant errors both near the occluding contour and over a large portion of object area bounded on one side by the shadow boundary with respect to illumination; for multiple images of a smooth dielectric object there will be significant viewpoint dependence of diffuse reflection for most object-viewpoint situations. Existing diffuse reflectance models for smooth surfaces do not account for these errors. In addition to experimentally verifying the viewpoint dependence of diffuse reflection, we show how the diffuse reflection maximum occurring between an occluding contour and the shadow boundary for a smooth dielectric illuminated by a point light source is accurately predicted because of this viewpoint dependence. For illumination incident at 90^o and greater relative to viewing, a diffuse reflection maximum is not even predicted by existing models having dependence only on angle of incidence, when in fact this maximum is very prominent. Furthermore, diffuse reflection is empirically observed to be very small in the immediate vicinity of an occluding contour for *all* illumination conditions, an observation that is not supported by existing models, and yet accounted for by expression 1.

A number of papers from the optics community have studied reflectance and transmission of light from diffuse scattering within dielectric media [12], [14], [16], [1], [5]. Some of these papers have presented theories for both reflectance and transmission for arbitrary optical thicknesses of scattering media, using collimated or diffuse light sources. In relation to the optics literature, this paper studies the specific case of diffuse reflectance from a semi-infinite, plane-parallel, inhomogeneous dielectric, which is most relevant to diffuse reflection observed in computer vision (and computer graphics). We assume that individual scattering of light from inhomogeneities within the dielectric medium is isotropic. The assumption that the scatterers are isotropic stems from the observed physical characteristic of common smooth dielectric surfaces that diffuse reflectance is independent of azimuth about the surface normal with respect to viewing. Chandrasekhar [3], whose derivation we utilize for the subsurface scattering distribution, shows that azimuth symmetric distributions arise from multiple scattering only when individual scatterers produce an isotropic distribution.

It should be emphasized that non-Lambertian diffuse reflection discussed in this paper is *distinct* from the specular component arising purely from surface interface reflection, such as described in the works by Torrance and Sparrow [21], and, Beckmann and Spizzichino [2]. Only very recently has there been consideration of non-Lambertian diffuse reflection within the vision and graphics community. Healey derives an expression for diffuse reflection based on Reichman's model for the semi-infinite case of opaque dielectrics [8], [7] applying this to geometry insensitive color segmentation. Tagare and deFigueiredo [20] propose as part of their multiple lobed reflectance model for machine vision a functional approximation to the Chandrasekhar diffuse reflection Law [3] for application to photometric stereo. While we also use the Chandrasekhar diffuse reflection law for diffuse subsurface scattering, it is not nearly accurate for materials without consideration of various dielectric-air boundary effects. Oren and Nayar [15] have proposed a diffuse reflection model for very rough dielectric surfaces assuming a

statistical distribution of Lambertian reflecting facets along with masking, shadowing, and, intereflection. The mechanism of using roughness elements that are assumed to be Lambertian however implies that in the limit as surface roughness gets smaller and smaller, that smooth surfaces therefore have Lambertian behavior- a phenomenon shown to be largely not true. In the Conclusion section, suggestions are made on how to possibly combine these two models to produce a unified model that accurately predicts diffuse reflection throughout the entire range of very rough to smooth surfaces.

Apart from analysis of reflected intensity distributions for diffuse reflection, Shafer [17] proposed a *dichromatic* color reflectance model for diffuse and specular components, and Wolff [22] proposed a polarization reflectance model involving the diffuse reflection component for inhomogeneous dielectrics.

2 The Physics Of Diffuse Reflection From Multiple Scattering

The analysis of diffuse reflection in this paper begins with the theory of radiative transfer developed by Chandrasekhar [3] for multiple scattering of incident light upon stellar and planetary atmospheres. The important problem of diffuse reflection and transmission from plane parallel atmospheres in astrophysics has a number of similarities with diffuse reflection from inhomogeneous dielectric materials. Incident light strikes gaseous molecules within an atmosphere whereupon some of the light is absorbed, and some of the light is scattered with an assumed intensity distribution respective to each individual molecule. Similarly, particles forming discontinuities in refractive index within a dielectric absorb and scatter light that has penetrated the surface boundary, and this process can be quantified using radiative transfer theory.

The fundamentals of single scattering theory were established by Lord Rayleigh for particles smaller than the wavelength of incident light and by Mie for spherical particles of arbitrary size [10], [11]. It is commonly assumed that the scattered light produced by a single small particle has an axial symmetric scattered energy distribution about the incident direction of light. The angular distribution of the scattered radiation is described by a *phase function* $P(cos\theta)$ where θ is the scattering angle of deflection away from the direction of the incident light. See Figure 2. The function $P(cos\theta)/4\pi$ represents the proportion of incident light energy flux that is scattered into a given direction per unit solid angle. The proportion of total light energy flux that is reradiated (i.e., scattered) is given by:

$$\int_{unit\ sphere} P(\cos\theta)\frac{d\omega}{4\pi} = \rho \leq 1\,, \tag{2}$$

and ρ is referred to as the *single scattering albedo*. In nonconservative cases when $\rho < 1$ some energy is absorbed by the particle. The single scattering albedo is commonly wavelength dependent which accounts for the colored appearance of many dielectrics when illuminated by white light.

Materials for which $P(\cos\theta)$ is independent of θ allow a tractable physical analysis. Chandrasekhar's theory [3] would imply that for these materials the

diffuse reflection distribution is symmetric about the surface's azimuth. Such materials include many common materials like plastics, ceramics, rubber, opaque glasses and smooth glossy paints. The details of Chandrasekhar's diffuse reflection law are explained in [24].

3 Diffuse Reflection From Smooth Dielectrics

Chandrasekhar's theory can be adapted so as to account for diffuse reflection from smooth inhomogeneous dielectric materials made up of particle inhomogeneities embedded in a medium with uniform index of refraction different from that of air. Once adapted the theory permits useful expressions that quantify the process of diffuse reflection from such materials. These expressions are summarized in this section, with the full technical derivations and details described in [24].

The first-order expression for diffuse reflection [23] quantifies reflection caused by light that penetrates into the material surface, scatters amongst sub-surface particle inhomogeneities, and then refraction back out into air. See Figure 1. This expression is given by:

$$\varrho_1 L \times [1 - F(\psi, n)] \times \cos\psi \times [1 - F(\overline{\phi}, 1/n)] d\omega \,,$$

for light incident at radiance L through solid angle $d\omega$. The functions, $F(,)$, are the Fresnel reflection coefficients [18] as functions of specular angle (external angle of incidence ψ for the first $F(,)$, and internal angle of incidence $\overline{\phi}$ for the second $F(,)$), and, index of refraction (n for light incident on the dielectric interface from air external to the dielectric for the first $F(,)$, and $1/n$ for light incident on the dielectric interface internal to the dielectric for the second $F(,)$). The internal angle $\overline{\phi}$ is related to the angle of emittance, ϕ using Snell's Law, $\overline{\phi} = \sin^{-1}(\frac{\sin\phi}{n})$. The term

$$\varrho_1 = \frac{\rho}{4\pi n^2} \frac{H_\rho(\overline{\mu}_{inc}) H_\rho(\overline{\mu}_{ref})}{\overline{\mu}_{inc} + \overline{\mu}_{ref}}, \quad \overline{\mu}_{inc} = \sqrt{1 - \frac{\sin^2\psi}{n^2}}, \quad \overline{\mu}_{ref} = \sqrt{1 - \frac{\sin^2\phi}{n^2}}$$

using the Chandrasekhar H-function is termed the *first-order diffuse albedo* as it represents the scaling of diffuse reflection magnitude. An Nth order approximation to the Chandrasekhar H-function [3] can be expressed;

$$H_\rho(\mu) \;=\; \frac{1}{\mu_1 \cdots \mu_n} \frac{\prod_{i=1}^{N}(\mu + \mu_i)}{\prod_\alpha (1 + \kappa_\alpha \mu)} \,,$$

defined in terms of the positive zeros, μ_i, of the even Legendre polynomial of order $2N$, and the positive roots, κ_α, of the associated *characteristic equation*;

$$1 \;=\; \sum_{j=1}^{N} \frac{a_j \rho}{1 - \kappa^2 \mu_j^2} \,.$$

Upon refraction from inside the dielectric into air at the dielectric interface, there can be significant specular reflection back into the dielectric. This produces

additional sub-surface scattering resulting in a second refraction back out into air, in turn resulting in specular reflection back into the dielectric, and so on. The contribution of Nth order diffuse reflection resulting from light that has been internally specularly reflected at the dielectric interface $N-1$ times and subsurface diffusely scattered N times (the first subsurface diffuse scattering before the first internal reflection) is given by:

$$\varrho_1 L \times [1 - F(\psi, n)] \times \cos\psi \times K^{N-1} \times [1 - F(\overline{\phi}, 1/n)] d\omega \,,$$

where

$$K = \int_0^{\pi/2} F(\phi', 1/n)\, C_\rho(\cos\phi', \sqrt{1 - \frac{\sin^2\phi}{n^2}}) 2\pi \sin\phi' d\phi' \,,$$

with

$$C_\rho(x, y) = \frac{\rho}{4\pi} L \frac{x}{x+y} H_\rho(x) H_\rho(y) \,,$$

The total amount of diffuse reflection is obtained by summing all Nth order contributions resulting in the expression:

$$\varrho L \times [1 - F(\psi, n)] \times \cos\psi \times [1 - F(\overline{\phi}, 1/n)] d\omega \tag{3}$$

$$\varrho = \sum_{i=1}^{\infty} \varrho_1 \times K^{i-1} = \frac{\varrho_1}{1-K} \,, \tag{4}$$

and ϱ is termed the *total diffuse albedo*. What is important to note is that the total diffuse albedo can be expressed purely in terms of physical parameters of the dielectric.

The assumptions made in the derivation of expression 3 are summarized in Table I below:

ASSUMPTION	COMMENTS
Isotropic Single Scattering	Azimuth independent diffuse reflection distribution
Uniform Distribution of Scattering Particles	Plane parallel uniformity of particles embedded in dielectric medium of uniform index of refraction. Able to apply Chandrasekhar theory.
Smooth Surface	Able to use Fresnel Coefficients, $F(,)$
Unpolarized Incident Light	Can be generalized to any incident polarization state using combination of $F_\parallel$ and $F_\perp$ terms
ρ_1 is constant	Very nearly true for all geometries to within 3%
K is constant	Very nearly true due to near isotropy of $C_\rho(,)$ for significant single scattering albedo, ρ

TABLE I

4 Experimental Results

Figure 3 shows an experimental goniometer apparatus that we built to measure diffuse reflected radiance from an optically smooth piece of white magnesium oxide ceramic, for different combinations of angles of incidence and emittance in the plane horizontal to the floor.

Figures 3 and 4 show experimental results for diffuse reflection from an optically smooth piece of white magnesium oxide ceramic. The magnesium oxide ceramic was measured with a stylus profilometer to have a variation in height profile no greater than half the wavelength of green light. The measurements were taken with a Panasonic CCD linear camera mounted at the end of a goniometer arm with the sample mounted at the center. Using a Brewster angle technique [4] the index of refraction of the ceramic was determined to be $n = 1.7$. Our diffuse reflectance model enables the empirical measurement of the single scattering albedo, ρ, by empirically determining the ratio of the strengths of the specular and diffuse components of reflection at known angles of incidence and emittance. The ratio of the specular to the diffuse reflection component was measured very near normal incidence and emittance and compared with the ratio:

$$\frac{F(0,n)}{\varrho(1-F(0,n))(1-F(0,1/n))d\omega},$$

where the total diffuse albedo ϱ is given by expression 4, and $d\omega$ is the solid angle in steradians subtended by the illuminating light source. The value of ϱ can be derived from this, and in turn, ρ can be computed by observing the graphed relationship between ρ and ϱ in Figure 5. The empirically determined specular to diffuse ratio is accounted for by a single scattering albedo, ρ, just above 0.95 which is very energy conserving.

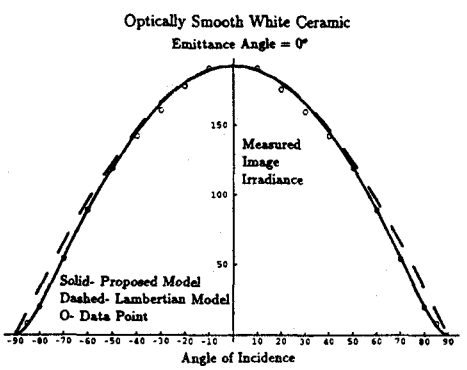

Figure 3

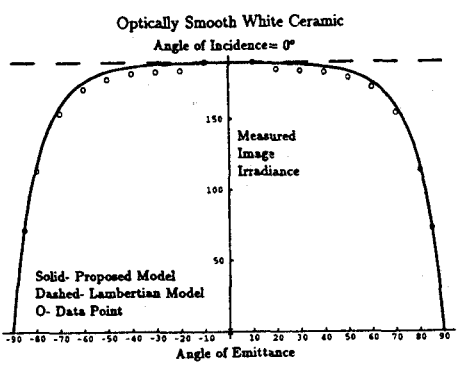

Figure 4

In Figures 3 and 4 dashed curves represent predicted Lambertian diffuse reflection, solid curves represent the diffuse reflection law of expression 3 with single scattering albedo $\rho = 0.95$ and index of refraction $n = 1.7$ (it makes little

difference for $1.0 \geq \rho \geq 0.9$, $1.4 \geq n \geq 2.0$ with respect to the shape of the diffuse reflection curve). The proposed diffuse reflection law, expression 3, never deviates more than 3% from the empirical data while there exist large deviations from Lambertian behavior. The results show that the Lambertian model can be assumed to within about 5% accuracy if angle of incidence and angle of emittance are simultaneously no larger than 50^o. Outside of this constraint range large deviations start to occur.

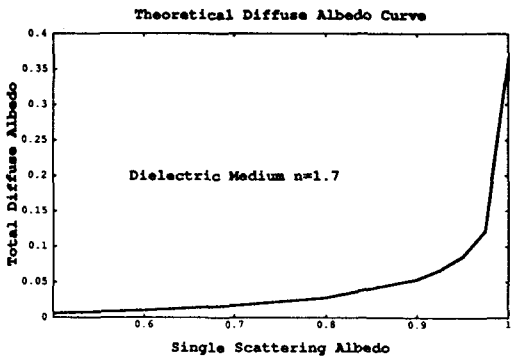

Figure 5: Graph of ϱ versus ρ using expression (4).

Figure 6 shows an ordinary scene where the Lambertian model strikingly breaks down altogether and yet is explained with high accuracy by the proposed diffuse reflection model in this paper. A ceramic coffee cup of cylindrical body shape is illuminated from the left side by an approximate point source. Starting from the left occluding contour going right the angle of incidence starts at 0^o and increases. The Lambertian model predicts that image intensities should decrease going to the right. The image intensities in fact increase to a maximum intensity at about 65^o surface orientation and then begin to slowly decrease. The reason is because, $\phi = 90^o - \psi$, that is the emittance angle starts at 90^o at the occluding contour and decreases going right. Looking at the graph in Figure 6a diffuse reflected radiance increases sharply as angle of emittance decreases from 90^o. At about surface orientation 65^o ($\psi = 25^o, \phi = 65^o$) the decrease of diffuse reflected radiance with respect to increasing angle of incidence starts to overtake the increase of diffuse reflected radiance with respect to decreasing angle of emittance, and a maximum occurs. (Note the graph in Figure 6a is only for the diffuse component and does not include measurement of the specular component which occurs at relative orientation 45^o in the picture of the cup.) According to Figure 6a the qualitative shape of the true diffuse reflected radiance curve (solid) is entirely different (e.g., its not even monotonic) from that for the Lambertian model (dashed). The deviation from the Lambertian model is also very high for frontal surface orientations where the angle of incidence is large. This non-Lambertian behavior of diffuse reflection occurs for a large range of lighting configurations as can be seen in Figure 6c with light source incident at 60^o relative to viewing (the diffuse reflection maximum occurs at about -50^o as predicted by the proposed model instead of -60^o as predicted by the Lambertian model, and note

the extreme drop in grey values going towards the occluding contour), and in Figure 6d with light source incident at 120° relative to viewing. For light incident at 90° or greater, Lambert's model as well as other existing diffuse reflectance models predict a monotonic diffuse reflection distribution which is empirically significantly incorrect.

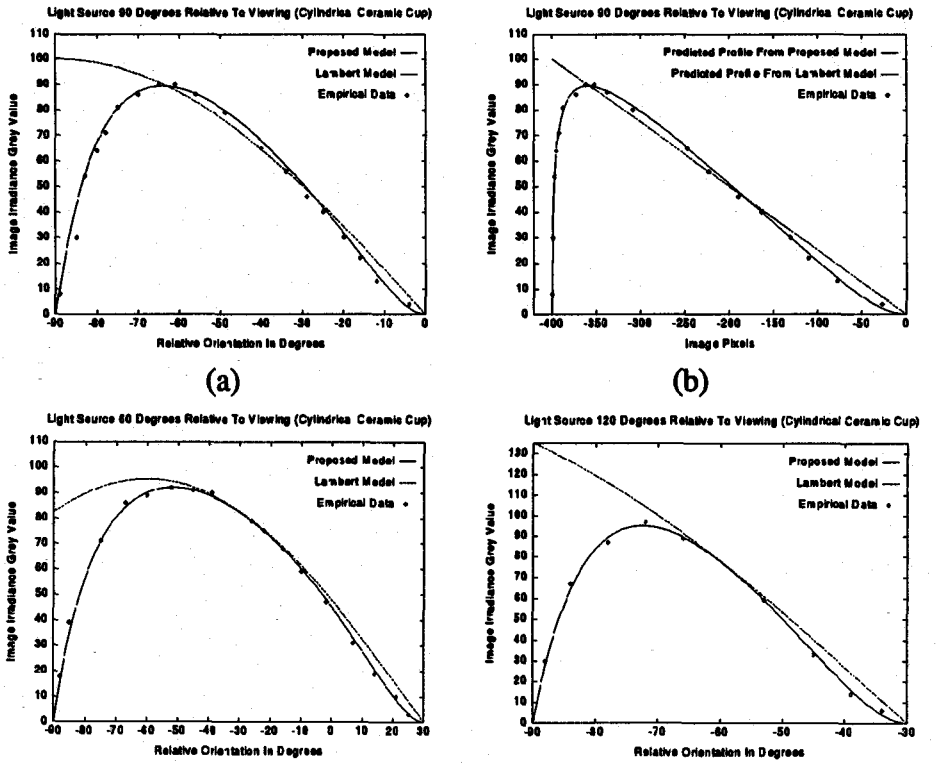

Figure 6

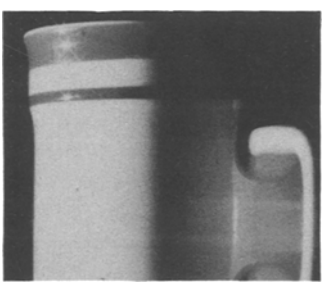

Note in Figure 6 that the leftmost portion of the cup visually looks relatively bright. It is however hard to tell from the photograph that instead of the brightness values at the occluding contour going crisply from the brightest value down to zero like a step-edge as predicted by Lambert's Law, that in fact the occluding

contour edge is "blurred" over a region the size of about 10% of the radius of the cup. This is precisely predicted by our diffuse reflectance model. Figure 6b shows the brightness profile predicted by our diffuse reflection model graphed spatially across a cylinder in pixel units where the center of the cylinder is at 0 on the horizontal axis and the occluding contour is at −400 on the horizontal axis. The experimental data in Figure 6b is consistent with this profile. (Note that Lambert's law predicts a linear diffuse reflection profile across an image in this case.) Due to foreshortening, the maximum brightness value occurring at 65^o relative surface orientation is about 10% of the radius of the cylinder away from the occluding contour. Between the point at which the brightness maximum occurs and the occluding contour, the brightness decreases to zero. While the brightness at the occluding contour is zero, due to the steepness of the profile shown in Figure 6b, the immediate vicinity of the occluding contour still has a relatively bright visual appearance. This is however instead of a step-edge between the occluding contour and the background. Thus occluding contour edge profiles for oblique lighting have the appearance of being blurred, and significantly displaced toward the interior of the object. With the same camera used to measure the profile in Figure 6b we have observed empirical step-edge profiles of a bright strip against a dark background that are localized to within about 2 or 3 pixels. Hence this effect at occluding contours from diffuse reflection for oblique lighting can be distinguished from typical lens blurring of step-edges as long as 10% of the radius of curvature near the occluding contour in pixel units is significantly larger than 2 or 3 pixels. Precise quantitative knowledge from our model of the brightness profile of occluding contour edges may aid in better determination of where the occluding contour is located in an image. The larger the cylinder radius (i.e., in general the larger the radius of curvature at the occluding contour) the more blurred and displaced will be the occluding contour edge defined by the profile of brightness values.

Figure 7a shows a real image of a white billiard ball illuminated by two point light sources orthogonal to viewing, one from the left side and one from the right side. Figure 7b shows a computer graphics rendering of a sphere illuminated by the same configuration of 2 point light sources assuming Lambert's diffuse reflectance law, while Figure 7c shows the same computer graphics rendering of a sphere using the diffuse reflectance law proposed in this paper. While both shadow boundaries with respect to the left and right light sources coincide along the vertically oriented great circle at the front of the sphere, there appears to be a "shadow band" of darker (i.e., smaller) intensity values about this shadow boundary due to the high fall off of diffuse reflectance at high angles of incidence near 90^o. Observe that realistically this "shadow band" is in fact significantly wider in Figure 7a than predicted by the Lambert Law in Figure 7b, but more accurately predicted by the proposed diffuse reflectance law in Figure 7c.

Figures 8a, 8b, and 8c show grey level representations of isophote curves (i.e., image curves with equal intensity) corresponding respectively to Figures 7a, 7b, 7c. Lambert's Law predicts for this configuration of light sources illuminating a sphere that equal reflected radiance occurs for points forming concentric cir-

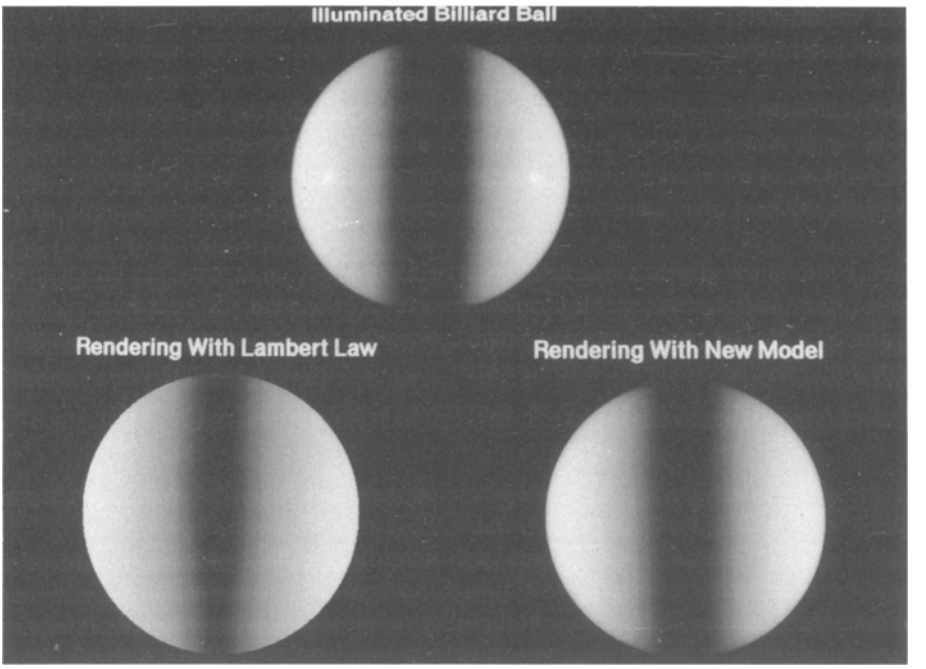

Figure 7 (Starting at top and going counterclockwise, 7a, 7b, 7c)

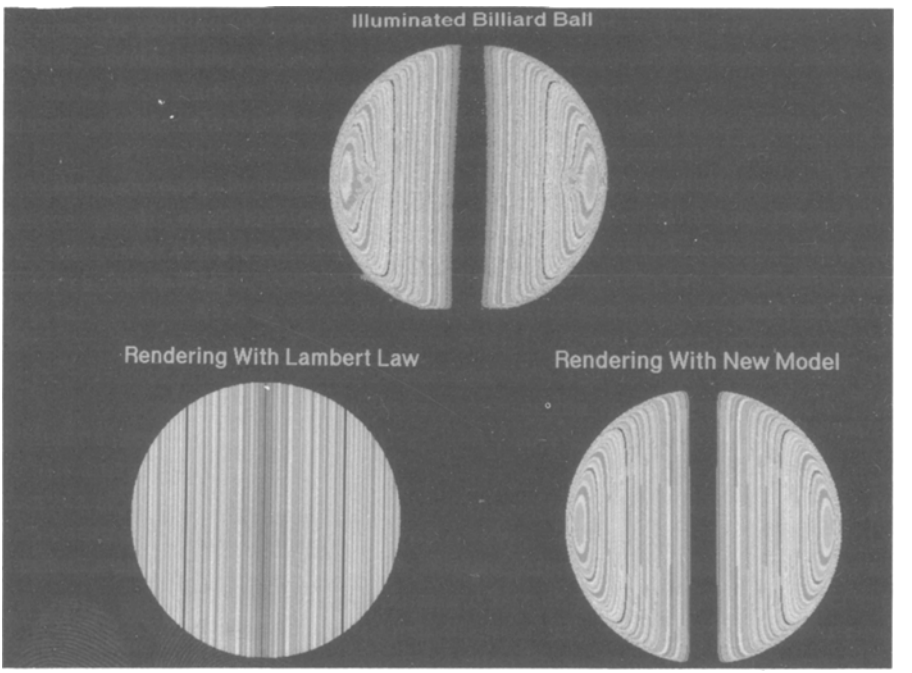

Figure 8 (Starting at top and going counterclockwise, 8a, 8b, 8c)

cles on the sphere about the left-most and right-most occluding contour points. These concentric circles of equal reflected radiance orthographically project onto straight isophote lines as depicted in Figure 8b, with maximum diffuse reflectance occurring at the left-most and right-most occluding contour points where the angle of incidence is zero. Figure 8a which is an actual depiction of the isophotes of Figure 7a shows that in fact lines of equal image intensity severely curve near the occluding contour of the sphere. Maximum diffuse reflection occurs at the center of the closed elliptical isophotes near the left-most and right-most occluding contours while diffuse reflection at the occluding contours is nearly zero, illustrating a 2-dimensional version of the effect depicted in Figure 6a. Figure 8c shows the isophotes rendered using the diffuse reflectance model proposed in this paper which are remarkably similar to the actual isophotes in Figure 8a (except for the isophotes perturbed by the specularities). Comparing Figures 8a, 8b, 8c shows very clearly how our diffuse reflectance model accurately predicts reflectance features that are significantly deviant from Lambertian behavior.

5 Conclusion

The primary result of this paper is a simple closed form expression, (equation 3 and equation 4), derived from first physical principles which accurately characterizes diffuse reflection from smooth dielectric surfaces exhibiting azimuth independent diffuse reflection about the surface normal with respect to viewing. In computer vision and computer graphics the Lambert diffuse reflection law has been almost always assumed for diffuse reflecting dielectric surfaces. Our diffuse reflection model shows that Lambert's Law is a good approximation across illuminated smooth dielectric objects when the angle of incidence and angle of emittance are simultaneously less than 50^o at each object point- and that there are significant deviations from Lambertian behavior for illumination-object-viewer geometries outside of this range. For oblique lighting of objects some strikingly non-Lambertian effects have been demonstrated that occur for common smooth dielectric surfaces, that are very accurately explained by this new diffuse reflectance model. An improved algorithm for the stereo matching of intensities is described in [26] accounting for this behavior. Our proposed diffuse reflection model has the added feature that it explains the physical origin of diffuse albedo, ϱ, (equation 4), which is typically an *ad hoc* scaling coefficient. This can be used to explain the relative strengths of the specular and diffuse reflection components from smooth inhomogeneous dielectric surfaces purely in terms of the physical parameters of the surface itself as shown in [25].

The proposed model for diffuse reflectance from smooth surfaces gives significant insight into generalizing a diffuse reflection model for different levels of roughness. In particular, modeling the local geometry of rough surfaces as a collection of smooth microfacets each having the diffuse reflectance property proposed in this paper (in lieu of the Lambertian model used in [15]) makes the limiting case of diffuse reflection as surface roughness goes towards zero accurate, while simultaneously having the large potential of accurately predicting diffuse reflection from intermediate ranges of surface roughness. If closed form expressions for diffuse reflection can be obtained from such a model, this would

be applicable to the entire range of rough to smooth surfaces and would be a further significant advancement.

References

1. J.R. Aronson and A.G. Emslie. Spectral reflectance and emittance of particulate materials. 2: Application and results. *Applied Optics*, 12(11):2573–2584, November 1973.
2. P. Beckmann and A. Spizzichino. *The Scattering of Electromagnetic Waves from Rough Surfaces.* Macmillan, 1963.
3. S. Chandrasekhar. *Radiative Transfer.* Dover Publications, New York, 1960.
4. D. Clarke and J.F. Grainger. *Polarized Light and Optical Measurement.* Pergamon Press, 1971.
5. A.G. Emslie and J.R. Aronson. Spectral reflectance and emittance of particulate materials. 1: Theory. *Applied Optics*, 12(11):2563–2572, November 1973.
6. W.E.L. Grimson. Binocular shading and visual surface reconstruction. *Computer Vision Graphics and Image Processing*, 28(1):19–43, 1984.
7. G. Healey. Using color for geometry-insensitive segmentation. *Journal of the Optical Society of America A*, 6(6):920–937, June 1989.
8. G. Healey and T.O. Binford. The role and use of color in a general vision system. In *Proceedings of the DARPA Image Understanding Workshop*, pages 599–613, Los Angeles, California, February 1987.
9. B.K.P. Horn and M.J. Brooks. *Shape From Shading.* MIT Press, 1989.
10. H.C. Van De Hulst. *Light Scattering by Small Particles.* John Wiley and Sons, New York, 1957.
11. M. Kerker. *The Scattering of Light and other Electromagnetic Radiation.* Academic Press, 1969.
12. P. Kubelka and F. Munk. Ein beitrag sur optik der farbanstriche. *Z. tech.*, 12:593, 1931.
13. J. H. Lambert. Photometria sive de mensura de gratibus luminis, colorum et umbrae. *Augsberg, Germany: Eberhard Klett*, 1760.
14. S. Orchard. Reflection and transmission of light by diffusing suspensions. *Journal of the Optical Society of America*, 59(12):1584–1597, December 1969.
15. M. Oren and S. Nayar. *Seeing Beyond Lambert's Law.* Proceedings of the Third European Conference on Computer Vision (ECCV 1994), Stockholm, May 1994.
16. J. Reichman. Determination of absorption and scattering coefficients for nonhomogeneous media 1: Theory. *Applied Optics*, 12(8):1811–1815, August 1973.
17. S. Shafer. Using color to separate reflection components. *Color Research and Application*, 10:210–218, 1985.
18. R. Siegal and J.R. Howell. *Thermal Radiation Heat Transfer.* McGraw-Hill, 1981.
19. G.B. Smith. Stereo integral equation. In *Proceedings of the AAAI*, pages 689–694, 1986.
20. H.D. Tagare and R.J.P. deFigueiredo. A theory of photometric stereo for a general class of reflectance maps. In *Proceedings of the IEEE conference on Computer Vision and Pattern Recognition (CVPR)*, pages 38–45, San Diego, June 1989.
21. K. Torrance and E. Sparrow. Theory for off-specular reflection from roughened surfaces. *Journal of the Optical Society of America*, 57:1105–1114, 1967.
22. L.B. Wolff. *Polarization Methods in Computer Vision.* PhD thesis, Columbia University, January 1991.

23. L.B. Wolff. Diffuse reflection. In *Proceedings of IEEE Conference on Computer Vision and Pattern Recognition (CVPR)*, pages 472–478, Urbana-Champaign Illinois, June 1992.
24. L.B. Wolff. A diffuse reflectance model for smooth dielectrics. *Journal of the Optical Society of America, (JOSA) A, Special Issue on Physics Based Machine Vision*, 11(11):2956–2968, November 1994.
25. L.B. Wolff. Relative brightness of specular and diffuse reflection. *Optical Engineering*, 33(1):285–293, January 1994.
26. L.B. Wolff and E. Angelopoulou. *3-D Stereo Using Photometric ratios.* Proceedings of the Third European Conference on Computer Vision (ECCV 1994), Stockholm, May 1994.